

Quantum-information approach to the quantum phase transition in the Kitaev honeycomb modelJian Cui,^{*} Jun-Peng Cao, and Heng Fan*Institute of Physics, Chinese Academy of Sciences, Beijing National Laboratory for Condensed Matter Physics, Beijing 100190, China*

(Received 12 May 2010; published 16 August 2010)

The Kitaev honeycomb model with a topological phase transition at zero temperature is studied using the quantum-information method. Based on the exact solution of the ground state, the mutual information between two nearest sites and between two bonds with the greatest distance are obtained. It is found that the mutual information shows some singularities at the critical point where the system transits from the gapless phase to the gapped phase. Finite-size effects and scaling behavior are also studied. Our results indicate that the mutual information can serve as a good indicator of the topological phase transition. This is because the mutual information is believed to be able to catch some global correlation properties of the system. Meanwhile, this method has the advantages that the phase transition can be determined easily and the order parameters, which are hard to obtain for some topological phase transitions, are not necessarily known.

DOI: [10.1103/PhysRevA.82.022319](https://doi.org/10.1103/PhysRevA.82.022319)

PACS number(s): 03.67.-a, 05.70.Jk, 05.30.Pr, 75.10.Jm

I. INTRODUCTION

Recently, the Kitaev honeycomb model has become a popular subject in both the fields of condensed matter physics and quantum-information processing [1–13]. This model was first introduced by Kitaev to study anyons, and the analytic exact solution to the ground state of this model has been obtained by several methods [1,14–17]. It has rich phase transitions and has both a gapless phase with non-Abelian anyon excitation and three gapped phases with Abelian anyon excitations depending on the values of the parameters in the Hamiltonian. It has been shown that the system possess a topological phase transition, which cannot be characterized by symmetry-breaking theory and the corresponding local order parameters but can be characterized by nonlocal string order parameters [1,18]. One interesting point is that the system is a scarce exactly solvable model with dimension higher than one, and thus it provides a test bed for many numerical methods in two-dimensional systems just as the Ising model does in one dimension. With these interesting properties, the Kitaev honeycomb model has been studied intensively and has been extended to other cases [12,19].

The Kitaev honeycomb model also has practical advantages as an active subject potential applications in quantum information and quantum computation. It has been suggested to use the Kitaev honeycomb model to realize fault-tolerant topological quantum computation. The system is a good candidate to encode quantum information while those quantum states can be naturally protected from the inevitable decoherence by the environment [20]. The Kitaev honeycomb model can be realized by using an optical lattice [21,22] and by using superconducting quantum circuits [23,24]. It has also been studied by means of fidelity susceptibility [15] and the extended Kitaev model has been studied with entanglement approaches [13].

In this paper, we investigate the Kitaev honeycomb model from the quantum-information perspective [25,26]. We study the topological phase transition in this model by means

of mutual information between the component lattices. It is generally believed that the mutual information measures the total information and describes the global correlation properties [27]. We find that both the derivative of mutual information between two nearest neighbor lattices and the mutual information between two bonds of the lattice can detect the topological phase transition in the Kitaev honeycomb model. This quantum-information method has great advantages in that the singular behavior occurs exactly at the point when the gapless phase transits into a gapped phase. We also study finite-size effects and the scaling behavior of the singularities of the mutual information.

This paper is organized as follows. In Sec. II we briefly introduce the Kitaev honeycomb model, then diagonalize the Hamiltonian and give the exact solution of the ground state based on Kitaev's initial method. After that, we calculate the two-site and four-site correlation functions to prepare for the determination of the two-site and two-bond reduced density matrix. In Secs. III and IV, we calculate the two-site mutual information and two-bond mutual information and the former one's derivative, respectively. Section V gives conclusions and remarks.

II. KITAEV HONEYCOMB MODEL

The Kitaev honeycomb model is a two-dimensional spin-1/2 lattice model with nearest neighbor interactions. It has two kinds of simple sublattices, which are denoted by the dark dots and empty circles in Fig. 1. Each lattice interacts with three nearest neighbors of the opposite kind through three distinct bonds labeled as an x link, a y link, and a z link. For each bond the interaction has a different coupling constant. The Hamiltonian is

$$H = -J_x \sum_{x \text{ links}} \sigma_j^x \sigma_k^x - J_y \sum_{y \text{ links}} \sigma_j^y \sigma_k^y - J_z \sum_{z \text{ links}} \sigma_j^z \sigma_k^z, \quad (1)$$

where the subindexes j, k denote the location of the site, and σ_k^α ($\alpha = x, y, z$) is the Pauli matrix at site k . We take the axis of the system in the \mathbf{n}_1 and \mathbf{n}_2 direction, and in each direction there are L unit cells. Therefore the whole system has $2L^2$

^{*}cuijian@iphy.ac.cn

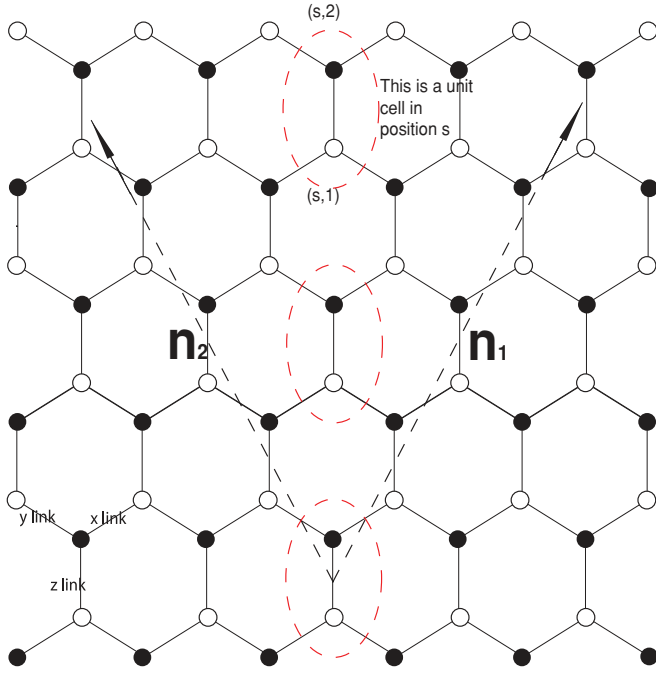


FIG. 1. (Color online) Sketch of the Kitaev honeycomb model. The unit cell (highlighted by an elliptic circle) contains two sites of different kinds. For simplicity, we choose the coordinate axes in \mathbf{n}_1 and \mathbf{n}_2 directions.

sites. Next, we use Kitaev's original method to diagonalize this Hamiltonian and get its ground state.

A. The ground state

We first introduce the following Majorana transformation to transform the Pauli operators into the Majorana fermion operators:

$$\sigma^x = ib^x c, \quad \sigma^y = ib^y c, \quad \sigma^z = ib^z c, \quad (2)$$

where the Majorana operators satisfy $A^\dagger = A$, $A^2 = 1$, $AB + BA = 0$, and $b^x b^y b^z c = 1$, for $A, B \in \{b^x, b^y, b^z, c\}$ and $A \neq B$. Thus, the Hamiltonian becomes

$$\begin{aligned} H &= - \sum_{\alpha} J^{\alpha} \sum_{\alpha \text{ links}} b_j^{\alpha} b_k^{\alpha} c_j c_k \\ &= i \sum_{\alpha} J^{\alpha} \sum_{\alpha \text{ links}} (i b_j^{\alpha} b_k^{\alpha}) c_j c_k \\ &= i \sum_{\alpha} J^{\alpha} \sum_{\alpha \text{ links}} \hat{u}_{jk} c_j c_k \\ &= \frac{i}{2} \sum_{j,k} J_{\alpha_{j,k}} \hat{u}_{j,k} c_j c_k. \end{aligned} \quad (3)$$

In the last equation, the value of α is totally determined by the site indexes j and k . The factor 1/2 is due to each lattice being counted twice in the summation of the lattices. It can be easily shown that $\hat{u}_{j,k}^2 = 1$, $[\hat{u}_{j,k}, H] = 0$, and $\hat{u}_{j,k}$ commute with each other. As a result the eigenvalues of $\hat{u}_{j,k}$ we present here by $u_{j,k}$ are ± 1 , and the whole Hilbert space can be decomposed into a series of eigenvalue spaces described by the eigenvalues of $\hat{u}_{j,k}$. According to Refs. [14,28], the

ground state is in the vortex-free space so that we assume $u_{j,k} = 1$ for all links, where j is a kind of simple sublattice presented by the empty circles in this paper. Notice that $u_{j,k} = -u_{k,j}$.

As the unit cell of this model contains one empty circle lattice and one dark dot lattice, we introduce a pair of indexes (\mathbf{s}, λ) to take the place of the previous site index j , where the first index \mathbf{s} stands for the location of the unit cell and the second one describes the two different kinds of sublattice. In this paper, we let the empty circle's second index take the value 1, and the dark dot's index takes the value 2. See Fig. 1. Then the Hamiltonian becomes

$$H = \frac{i}{2} \sum_{\mathbf{s}, \lambda, \mathbf{t}, \mu} J_{\mathbf{s}, \lambda, \mathbf{t}, \mu} c_{\mathbf{s}, \lambda} c_{\mathbf{t}, \mu}. \quad (4)$$

The two-dimensional system we studied is on the surface of a torus with periodic boundary conditions. Because of the translational invariance of the system, $J_{\mathbf{s}, \lambda, \mathbf{t}, \mu}$ is actually determined by three indexes: λ , μ , and $\mathbf{t} - \mathbf{s}$. Then we introduce the Fourier transformation

$$\begin{aligned} J_{\mathbf{s}, \lambda, \mathbf{t}, \mu} &= J_{0, \lambda; \mathbf{t} - \mathbf{s}, \mu} = \frac{1}{L^2} \sum_{\mathbf{q}} e^{-i\mathbf{q} \cdot (\mathbf{r}_t - \mathbf{r}_s)} \tilde{J}_{\lambda, \mu}(\mathbf{q}), \\ c_{\mathbf{s}, \lambda} &= \sqrt{\frac{2}{L^2}} \sum_{\mathbf{q}} e^{i\mathbf{q} \cdot \mathbf{r}_s} a_{\mathbf{q}, \lambda}. \end{aligned} \quad (5)$$

The inverse transformation is

$$\begin{aligned} \tilde{J}_{\lambda, \mu}(\mathbf{q}) &= \sum_{\mathbf{t}} e^{i\mathbf{q} \cdot \mathbf{r}_t} J_{0, \lambda; \mathbf{t}, \mu}, \\ a_{\mathbf{q}, \lambda} &= \sqrt{\frac{1}{2L^2}} \sum_{\mathbf{s}} e^{-i\mathbf{q} \cdot \mathbf{r}_s} c_{\mathbf{s}, \lambda}, \end{aligned} \quad (6)$$

where $a_{\mathbf{q}, \lambda}$ satisfies $a_{-\mathbf{q}, \lambda} = a_{\mathbf{q}, \lambda}^\dagger$, $a_{\mathbf{q}, \lambda}^2 = 0$, $[a_{\mathbf{q}, \lambda}, a_{\mathbf{q}, \mu}^\dagger]_+ \equiv a_{\mathbf{q}, \lambda} a_{\mathbf{q}, \mu}^\dagger + a_{\mathbf{q}, \mu}^\dagger a_{\mathbf{q}, \lambda} = \delta_{\mathbf{p}\mathbf{q}} \delta_{\lambda, \mu}$, and other anticommutators are all equal to zero. Then the Hamiltonian becomes

$$H = i \sum_{\mathbf{q}} \sum_{\lambda, \mu=1}^2 \tilde{J}_{\lambda, \mu}(\mathbf{q}) a_{-\mathbf{q}, \lambda} a_{\mathbf{q}, \mu}. \quad (7)$$

After simple calculations we obtain $\tilde{J}_{1,1}(\mathbf{q}) = \sum_{\mathbf{t}} e^{i\mathbf{q} \cdot \mathbf{r}_t} J_{01, \mathbf{t}1} = 0$, because $J_{01, \mathbf{t}1} = 0$. For a similar reason $\tilde{J}_{2,2}(\mathbf{q}) = 0$. As each lattice interacts with its three nearest neighbors, there are only three values of \mathbf{t} corresponding to the three neighbors that make $J_{01, \mathbf{t}2}$ take nonzero values. Thus $\tilde{J}_{1,2}(\mathbf{q}) = J_x e^{i\mathbf{q} \cdot \mathbf{n}_1} + J_y e^{i\mathbf{q} \cdot \mathbf{n}_2} + J_z$ and $\tilde{J}_{2,1}(\mathbf{q}) = -\tilde{J}_{1,2}^*(\mathbf{q})$, where \mathbf{n}_1 and \mathbf{n}_2 are in the directions shown in Fig. 1. Let $f(\mathbf{q}) \equiv \tilde{J}_{1,2}(\mathbf{q}) = \varepsilon(\mathbf{q}) + i\Delta(\mathbf{q})$, and choose \vec{q}_x to be in the direction of \mathbf{n}_1 and \vec{q}_y to be in the direction of \mathbf{n}_2 . Then we have

$$\begin{aligned} \varepsilon(\mathbf{q}) &= J_x \cos q_x + J_y \cos q_y + J_z, \\ \Delta(\mathbf{q}) &= J_x \sin q_x + J_y \sin q_y, \end{aligned} \quad (8)$$

where q_x and q_y take values $q_x, q_y = 2\pi n/L$, $n = -(L-1)/2, \dots, (L-1)/2$. We can see that $\varepsilon(-\mathbf{q}) = \varepsilon(\mathbf{q})$,

$\Delta(-\mathbf{q}) = -\Delta(\mathbf{q})$, and $f(-\mathbf{q}) = f^*(\mathbf{q})$. The Hamiltonian then becomes

$$H = \sum_{\mathbf{q}} i f(\mathbf{q}) a_{\mathbf{q},1}^\dagger a_{\mathbf{q},2} + [i f(\mathbf{q})]^* a_{\mathbf{q},2}^\dagger a_{\mathbf{q},1}. \quad (9)$$

Next, we introduce the following Bogoliubov transformation:

$$\begin{aligned} C_{\mathbf{q},1} &= u_{\mathbf{q}} a_{\mathbf{q},1} + v_{\mathbf{q}} a_{\mathbf{q},2}, \\ C_{\mathbf{q},1}^\dagger &= u_{\mathbf{q}}^* a_{\mathbf{q},1}^\dagger + v_{\mathbf{q}}^* a_{\mathbf{q},2}^\dagger, \\ C_{\mathbf{q},2} &= v_{\mathbf{q}}^* a_{\mathbf{q},1} - u_{\mathbf{q}}^* a_{\mathbf{q},2}, \\ C_{\mathbf{q},2}^\dagger &= v_{\mathbf{q}} a_{\mathbf{q},1}^\dagger - u_{\mathbf{q}} a_{\mathbf{q},2}^\dagger, \end{aligned} \quad (10)$$

with the new operators satisfying $[C_{\mathbf{q},\lambda}, C_{\mathbf{p},\mu}^\dagger]_+ = \delta_{\mathbf{p}\mathbf{q}} \delta_{\lambda,\mu}$, $C_{\mathbf{q},\lambda}^2 = 0$. By using the Bogoliubov transformation, the Hamiltonian is diagonalized as

$$H = \sum_{\mathbf{q}} |f_{\mathbf{q}}| (C_{\mathbf{q},1}^\dagger C_{\mathbf{q},1} - C_{\mathbf{q},2}^\dagger C_{\mathbf{q},2}), \quad (11)$$

with $u_{\mathbf{q}} = \frac{1}{\sqrt{2}}$, $v_{\mathbf{q}} = \frac{i}{\sqrt{2}} \frac{f_{\mathbf{q}}}{|f_{\mathbf{q}}|}$, $v_{-\mathbf{q}} = -v_{\mathbf{q}}^*$, and $C_{-\mathbf{q},1} = -2u_{\mathbf{q}}^* v_{\mathbf{q}}^* C_{\mathbf{q},2}^\dagger$. Since $C_{\mathbf{q},1}^\dagger C_{\mathbf{q},1} = 1 - C_{-\mathbf{q},2}^\dagger C_{-\mathbf{q},2}$, the Hamiltonian reads

$$\begin{aligned} H &= \sum_{\mathbf{q}} |f_{\mathbf{q}}| (1 - C_{-\mathbf{q},2}^\dagger C_{-\mathbf{q},2} - C_{\mathbf{q},2}^\dagger C_{\mathbf{q},2}) \\ &= \sum_{\mathbf{q}} |f_{\mathbf{q}}| (1 - 2C_{\mathbf{q},2}^\dagger C_{\mathbf{q},2}). \end{aligned} \quad (12)$$

The normalized ground state is

$$|G\rangle = \prod_{\mathbf{q}} C_{\mathbf{q},2}^\dagger |0\rangle, \quad (13)$$

with $C_{\mathbf{q},2} |0\rangle = 0$. The energy gap is $2 \min_{\mathbf{q}} \{|f_{\mathbf{q}}|\}$.

B. The phase diagram

This ground state has two distinct phases in the parameter space. In the region of $|J_x| \leq |J_y| + |J_z|$, $|J_y| \leq |J_x| + |J_z|$ and $|J_z| \leq |J_y| + |J_x|$ it is gapless with non-Abelian excitation, and in other regions it is gapped with Abelian anyon excitations [14]. We focus on the $J_x + J_y + J_z = 1$ plane. The phase diagram is shown in Fig. 2. In this paper, we investigate the behaviors of two-site mutual information and two-bond mutual information in the phase transition from the gapless phase to a gapped phase along the red dashed line in the phase diagram of Fig. 2.

C. Correlation functions

In this section we calculate the two-site and four-site correlation functions at the ground state of the systems that will be used to construct the reduced density matrix. Suppose the two nearest lattices to be studied are linked by z bonds. The correlation function between two nearest lattices is

$$\begin{aligned} \langle \sigma_{\mathbf{r},1}^z \sigma_{\mathbf{r},2}^z \rangle &= \left\langle b_{\mathbf{r},1}^z b_{\mathbf{r},2}^z \frac{2}{L^2} \sum_{\mathbf{q}, \mathbf{q}'} e^{i(\mathbf{q}+\mathbf{q}')\cdot\mathbf{r}} a_{\mathbf{q},1} a_{\mathbf{q}',2} \right\rangle \\ &= -i \frac{2}{L^2} \sum_{\mathbf{q}, \mathbf{q}'} e^{i(\mathbf{q}+\mathbf{q}')\cdot\mathbf{r}} \langle a_{\mathbf{q},1} a_{\mathbf{q}',2} \rangle. \end{aligned}$$

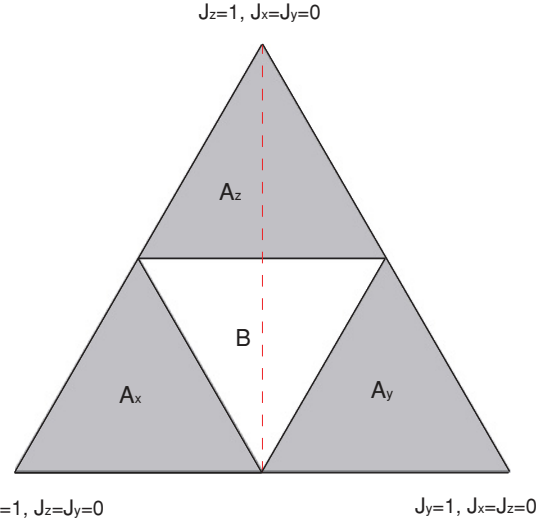


FIG. 2. (Color online) The phase diagram of the Kitaev honeycomb model in the $J_x + J_y + J_z = 1$ plane in the parameter space. In the three shaded areas labeled A_x , A_y , and A_z , the system is gapped with Abelian anyon excitation, and in the unshaded area labeled B the system is gapless with non-Abelian excitation. In this paper, we focus on the red dashed line $J_x = J_y = (1 - J_z)/2$, where the critical point of topological phase transition is $J_z = 0.5$.

By using the relation

$$\begin{aligned} \langle a_{\mathbf{q},1} a_{\mathbf{q}',2} \rangle &= \langle (u_{\mathbf{q}}^* C_{\mathbf{q},1} + v_{\mathbf{q}} C_{\mathbf{q},2})(v_{\mathbf{q}'}^* C_{\mathbf{q}',1} - u_{\mathbf{q}'} C_{\mathbf{q}',2}) \rangle \\ &= -u_{\mathbf{q}}^* u_{\mathbf{q}'} \langle C_{\mathbf{q},1} C_{\mathbf{q}',2} \rangle \\ &= \frac{i}{2} \delta_{\mathbf{q},-\mathbf{q}'} \frac{f_{\mathbf{q}}}{|f_{\mathbf{q}}|}, \end{aligned}$$

we obtain the correlation function

$$\begin{aligned} \langle \sigma_{\mathbf{r},1}^z \sigma_{\mathbf{r},2}^z \rangle &= \frac{1}{L^2} \sum_{\mathbf{q}} \frac{f_{\mathbf{q}}}{|f_{\mathbf{q}}|} = \frac{1}{2L^2} \sum_{\mathbf{q}} \frac{f_{\mathbf{q}} + f_{-\mathbf{q}}}{|f_{\mathbf{q}}|} \\ &= \frac{1}{L^2} \sum_{\mathbf{q}} \frac{\varepsilon_{\mathbf{q}}}{E_{\mathbf{q}}}, \end{aligned} \quad (14)$$

where $E_{\mathbf{q}} = |f_{\mathbf{q}}| = \sqrt{\varepsilon_{\mathbf{q}}^2 + \Delta_{\mathbf{q}}^2}$.

The correlation function between two bonds as highlighted by elliptic circles in Fig. 1 is

$$\begin{aligned} \langle \sigma_{\mathbf{r}_1,1}^z \sigma_{\mathbf{r}_1,2}^z \sigma_{\mathbf{r}_2,1}^z \sigma_{\mathbf{r}_2,2}^z \rangle &= \langle b_{\mathbf{r}_1,1}^z b_{\mathbf{r}_1,2}^z b_{\mathbf{r}_2,1}^z b_{\mathbf{r}_2,2}^z C_{\mathbf{r}_1,1} C_{\mathbf{r}_1,2} C_{\mathbf{r}_2,1} C_{\mathbf{r}_2,2} \rangle \\ &= -\frac{4}{L^4} \sum_{\mathbf{q}_1, \mathbf{q}_2, \mathbf{q}_3, \mathbf{q}_4} e^{i(\mathbf{q}_1+\mathbf{q}_2)\cdot\mathbf{r}_1} e^{i(\mathbf{q}_3+\mathbf{q}_4)\cdot\mathbf{r}_2} \\ &\quad \times \langle a_{\mathbf{r}_1,1} a_{\mathbf{r}_1,2} a_{\mathbf{r}_2,1} a_{\mathbf{r}_2,2} \rangle, \end{aligned}$$

where

$$\begin{aligned} \langle a_{\mathbf{r}_1,1} a_{\mathbf{r}_1,2} a_{\mathbf{r}_2,1} a_{\mathbf{r}_2,2} \rangle &= -\frac{1}{4} \frac{f_{\mathbf{q}_1}}{|f_{\mathbf{q}_1}|} \frac{f_{\mathbf{q}_3}}{|f_{\mathbf{q}_3}|} \langle C_{-\mathbf{q}_1,2}^\dagger (C_{-\mathbf{q}_2,2} + C_{\mathbf{q}_2,2}) \\ &\quad \times (C_{-\mathbf{q}_3,2}^\dagger - C_{\mathbf{q}_3,2}) C_{\mathbf{q}_4,2} \rangle \\ &= \frac{1}{4} \frac{f_{\mathbf{q}_1}}{|f_{\mathbf{q}_1}|} \frac{f_{\mathbf{q}_3}}{|f_{\mathbf{q}_3}|} (\delta_{\mathbf{q}_2,-\mathbf{q}_3} \delta_{\mathbf{q}_1,-\mathbf{q}_4} \\ &\quad - \delta_{\mathbf{q}_1,-\mathbf{q}_3} \delta_{\mathbf{q}_2,-\mathbf{q}_4} - \delta_{\mathbf{q}_1,-\mathbf{q}_2} \delta_{\mathbf{q}_3,-\mathbf{q}_4}). \end{aligned}$$

Then, we arrive at

$$\begin{aligned}
 \langle \sigma_{\mathbf{r}_1,1}^z \sigma_{\mathbf{r}_1,2}^z \sigma_{\mathbf{r}_2,1}^z \sigma_{\mathbf{r}_2,2}^z \rangle &= -\frac{1}{L^4} \left(\sum_{\mathbf{q}_1, \mathbf{q}_3} \frac{f_{\mathbf{q}_1}}{|f_{\mathbf{q}_1}|} \frac{f_{\mathbf{q}_3}}{|f_{\mathbf{q}_3}|} e^{i(\mathbf{q}_1 - \mathbf{q}_3) \cdot (\mathbf{r}_1 - \mathbf{r}_2)} - \sum_{\mathbf{q}_1, \mathbf{q}_2} e^{i(\mathbf{q}_1 + \mathbf{q}_2) \cdot (\mathbf{r}_1 - \mathbf{r}_2)} - \sum_{\mathbf{q}_1, \mathbf{q}_3} \frac{f_{\mathbf{q}_1}}{|f_{\mathbf{q}_1}|} \frac{f_{\mathbf{q}_3}}{|f_{\mathbf{q}_3}|} \right) \\
 &= -\frac{1}{L^4} \sum_{\mathbf{q}_1, \mathbf{q}_3} \frac{f_{\mathbf{q}_1} f_{\mathbf{q}_3} + f_{-\mathbf{q}_1} f_{-\mathbf{q}_3}}{|f_{\mathbf{q}_1}| \cdot |f_{\mathbf{q}_3}|} \{ \cos[(\mathbf{q}_1 - \mathbf{q}_3) \cdot (\mathbf{r}_1 - \mathbf{r}_2)] - 1 \} \\
 &= \frac{1}{L^4} \sum_{\mathbf{q}_1, \mathbf{q}_3} \frac{\Delta_{\mathbf{q}_1} \Delta_{\mathbf{q}_3} - \varepsilon_{\mathbf{q}_1} \varepsilon_{\mathbf{q}_3}}{E_{\mathbf{q}_1} E_{\mathbf{q}_3}} \{ \cos[(\mathbf{q}_1 - \mathbf{q}_3) \cdot (\mathbf{r}_1 - \mathbf{r}_2)] - 1 \}. \tag{15}
 \end{aligned}$$

III. MUTUAL INFORMATION BETWEEN TWO NEIGHBOR LATTICES

The reduced density matrix of two sites i and j is $\rho_{i,j} = \frac{1}{4} \sum_{\alpha, \beta=0}^3 \langle \sigma_i^\alpha \sigma_j^\beta \rangle \sigma_i^\alpha \sigma_j^\beta$, where $\sigma^1 = \sigma^x$, $\sigma^2 = \sigma^y$, $\sigma^3 = \sigma^z$, and σ^0 is the identity. In the system (1), each site interacts with its three neighbors by different operators (σ^x , σ^y , and σ^z), and each two linked sites together have only one kind of operator available (i.e., $\sigma^\alpha \sigma^\alpha$), with α corresponding to the type of their link. We find that only the correlation function along the link interacting direction is nonzero when we study the reduced matrix of two linked sites. That is, if we consider the two lattices with a z link (see Fig. 1), all the correlations are zero except $\langle \sigma^z \sigma^z \rangle$. Therefore, the reduced density matrix of this model has only diagonal elements, although the interactions of one site have three components. This indicates that the model (1) is much more like a classical system and similar to the Ising model. That may explain why this two-dimensional model can be solved analytically.

To show our results more clearly, we use a numerical method to diagonalize the Hamiltonian exactly. With the

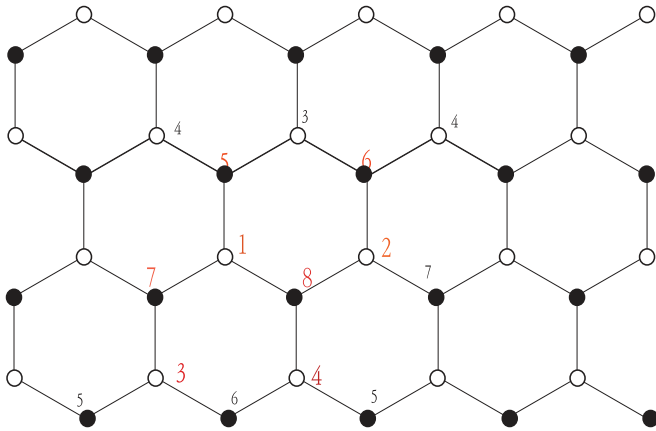


FIG. 3. (Color online) The smallest translation-invariant subsystem of the Kitaev honeycomb model with periodic boundary conditions. The eight interaction sites in the subsystem are highlighted by red numbers on the graph. The sites labeled by small black numbers are the repetitions of the eight sites because of the periodic boundary condition and torus topology.

periodic boundary conditions, we diagonalize an eight-lattice system, which is the smallest subsystem on the surface of a torus (see Fig. 3), and calculate all 16 two-site correlation functions. Here we omit the subindex corresponding to the sites' position because the value is invariant by the translational invariance of this system. The explicit form of the Hamiltonian reads

$$\begin{aligned}
 H_8 &= J_x (\sigma_5^x \sigma_3^x + \sigma_6^x \sigma_4^x + \sigma_7^x \sigma_1^x + \sigma_8^x \sigma_2^x) \\
 &\quad + J_y (\sigma_3^y \sigma_6^y + \sigma_5^y \sigma_4^y + \sigma_8^y \sigma_1^y + \sigma_7^y \sigma_2^y) \\
 &\quad + J_z (\sigma_3^z \sigma_7^z + \sigma_4^z \sigma_8^z + \sigma_5^z \sigma_1^z + \sigma_6^z \sigma_2^z). \tag{16}
 \end{aligned}$$

By using the periodic boundary conditions, the system size of the system (16) can be extended to infinity. The main properties of the system are kept since all possible interactions are considered. The result is shown in Fig. 4. We see that the correlation functions along the z direction are nonzero.

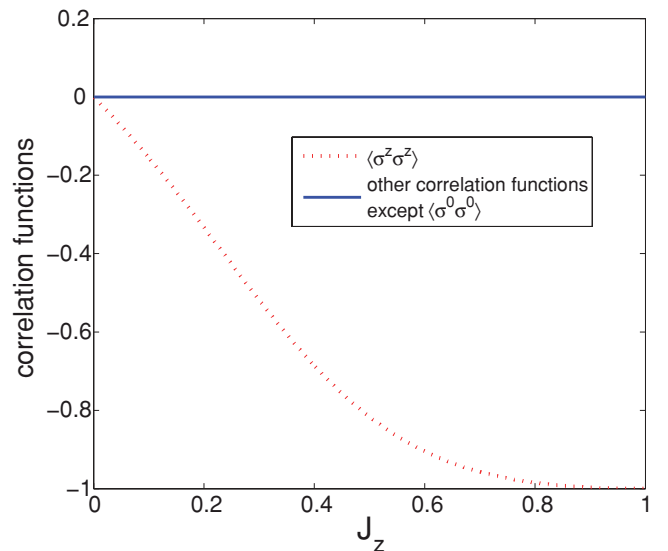


FIG. 4. (Color online) The ground-state two-site correlation functions with a z link in the Kitaev honeycomb model. We see that $\langle \sigma_{\mathbf{r}_1,1}^0 \sigma_{\mathbf{r}_2,2}^0 \rangle = 1$, $\langle \sigma_{\mathbf{r}_1,1}^z \sigma_{\mathbf{r}_2,2}^z \rangle \neq 0$, and others are zero. J_z is in units of $J_x + J_y + J_z$.

The explicit form of the reduced density matrix of two sites with a nearest neighbor is

$$\rho_{r,1;r,2} = \frac{1}{4} \begin{pmatrix} 1 + \langle \sigma_{r,1}^z \sigma_{r,2}^z \rangle & 0 & 0 & 0 \\ 0 & 1 - \langle \sigma_{r,1}^z \sigma_{r,2}^z \rangle & 0 & 0 \\ 0 & 0 & 1 - \langle \sigma_{r,1}^z \sigma_{r,2}^z \rangle & 0 \\ 0 & 0 & 0 & 1 + \langle \sigma_{r,1}^z \sigma_{r,2}^z \rangle \end{pmatrix}. \tag{17}$$

The eigenvalues of the reduced density matrix are $\lambda_1 = \lambda_2 = (1 - \langle \sigma^z \sigma^z \rangle)/4$ and $\lambda_3 = \lambda_4 = (1 + \langle \sigma^z \sigma^z \rangle)/4$. Every eigenvalue corresponds to two-fold degenerate eigenstates. From the two-site reduced density matrix we can derive the reduced density matrix for one site as $I/2$, where I is the identity matrix. The mutual information of the two sites i and j is

$$S(i : j) = 2 - 2H\left(\frac{1 - \langle \sigma^z \sigma^z \rangle}{4}\right) - 2H\left(\frac{1 + \langle \sigma^z \sigma^z \rangle}{4}\right), \tag{18}$$

where $H(x) = -x \log_2(x)$.

The two-site mutual information along the line $J_x = J_y = (1 - J_z)/2$ is shown in Fig. 5. We see that the mutual information increases monotonically with increasing J_z . However, there exists a certain value J_z^m for which if $J < J_z^m$, the mutual information is a concave function, whereas if $J > J_z^m$, the mutual information is a convex function. Thus, the first-order derivative of the mutual information with respect to J_z has a peak at J_z^m . J_z is in units of $J_x + J_y + J_z$.

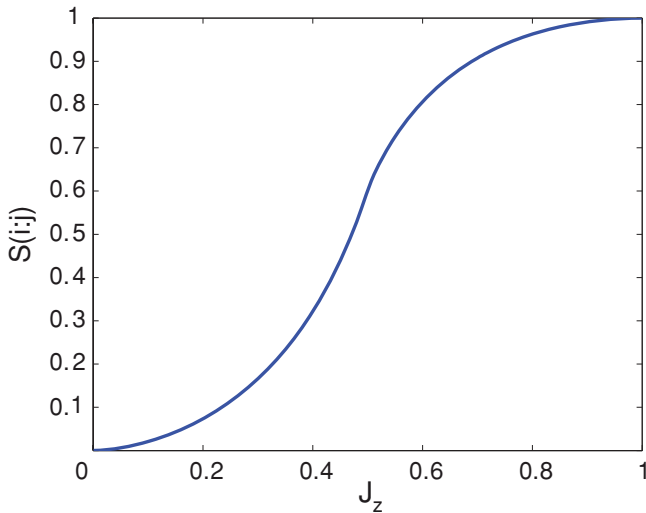


FIG. 5. (Color online) Mutual information between two connected sites. The mutual information increases monotonically with increasing J_z . However, there exists a certain value J_z^m for which if $J < J_z^m$, the mutual information is a concave function, whereas if $J > J_z^m$, the mutual information is a convex function. Thus, the first-order derivative of the mutual information with respect to J_z has a peak at J_z^m . J_z is in units of $J_x + J_y + J_z$.

the mutual information is a concave function whereas if $J > J_z^m$, the mutual information is a convex function. Thus, the first-order derivative of the mutual information with respect to J_z has a peak at J_z^m . The derivative of the mutual information is shown in Fig. 6. From Fig. 6, we see that the first-order derivative of the mutual information arrives at the maximum value at the point $J_z^m = 0.5$, which exactly corresponds the critical point $J_z = 0.5$. We also find that the value of J_z^m is fixed when the system size changes. The maximum value is a constant when the system size tends to infinity, as shown in Fig. 7. This is different from the Ising model, where the second-order derivative of entanglement entropy diverges at the critical point in the thermodynamic

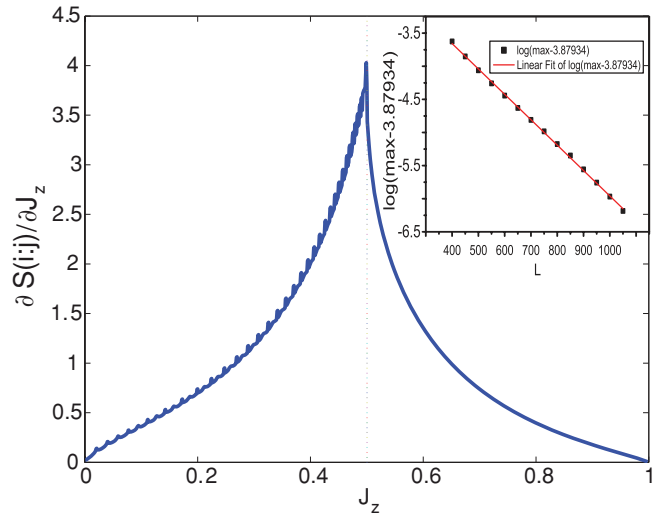


FIG. 6. (Color online) The first-order derivative of mutual information between two connected sites for system size $L = 100$. The derivative of the mutual information has a maximum exactly at the critical point $J_z = 0.5$. The small peaks in the gapless region result from the fact that while calculating $\langle \sigma_{r,1}^z \sigma_{r,2}^z \rangle$ certain ϵ_q and E_q are both infinitesimal and some systematic error is included. The peaks get smaller when L increases. The subgraph shows that when the system size tends to infinity, the maximum of the derivative of the mutual information tends to a constant as $\log_2[(\frac{\partial S(i:j)}{\partial J_z})_{\max} - 3.87934] = -0.00384L - 2.12174$. J_z is in units of $J_x + J_y + J_z$.

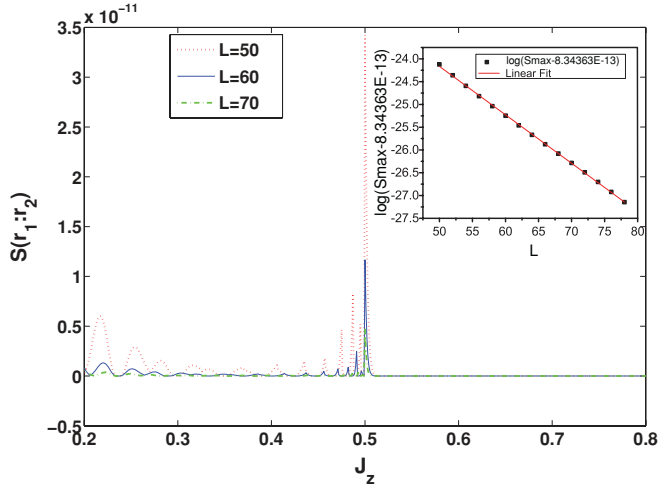


FIG. 7. (Color online) The mutual information between two z linked bonds with the greatest distance located on the torus surface for a given system size. The small peaks in the gapless phase are caused by the 0/0 error as before. The significant peak arises exactly at the critical point. The subgraph shows that when the system size tends to infinity, the peak value of the mutual information tends to a constant as $\log_2[S(\mathbf{r}_1 : \mathbf{r}_2)_{\max} - 8.34363 \times 10^{-13}] = -0.10637L - 18.8454$. Here J_z is in units of $J_x + J_y + J_z$.

limit [29], although their density matrices are the same in structure.

From the quantum-information perspective, the entanglement measured by concurrence between two sites is zero since the density has only diagonal elements, whereas the entanglement between one site and all the remaining sites is maximum [i.e., $c = \sqrt{\frac{d}{d-1}(1 - \text{Tr}\rho_i^2)} = 1$, where c denotes the concurrence, ρ_i is the reduced density matrix of the particle in site i , and d is the dimension of ρ_i] [30,31].

IV. MUTUAL INFORMATION BETWEEN TWO BONDS WITH LONGEST DISTANCE

In this section, we investigate the mutual information between two z linked bonds. First, we need to calculate the density matrix. For two arbitrary z linked bonds at \mathbf{r}_1 and \mathbf{r}_2 the density matrix is

$$\rho_{\mathbf{r}_1, \mathbf{r}_2} = \frac{1}{16} \sum_{\alpha, \beta=0,3} \sigma_{\mathbf{r}_1,1}^\alpha \sigma_{\mathbf{r}_1,2}^\alpha \sigma_{\mathbf{r}_2,1}^\beta \sigma_{\mathbf{r}_2,2}^\beta \langle \sigma_{\mathbf{r}_1,1}^\alpha \sigma_{\mathbf{r}_1,2}^\alpha \sigma_{\mathbf{r}_2,1}^\beta \sigma_{\mathbf{r}_2,2}^\beta \rangle. \quad (19)$$

The eigenvalues of this density matrix are $(1 - 4\langle \sigma^z \sigma^z \sigma^z \sigma^z \rangle)/16$, $(1 - 2\langle \sigma^z \sigma^z \rangle + \langle \sigma^z \sigma^z \sigma^z \sigma^z \rangle)/16$, and $(1 + 2\langle \sigma^z \sigma^z \rangle + \langle \sigma^z \sigma^z \sigma^z \sigma^z \rangle)/16$. These eigenvalues correspond to eight-fold, four-fold, and four-fold degenerate eigenstates, respectively. Then we obtain the mutual information between two z linked bonds in \mathbf{r}_1 and \mathbf{r}_2 as

$$S(\mathbf{r}_1 : \mathbf{r}_2) = 4H\left(\frac{1 + \langle \sigma^z \sigma^z \rangle}{4}\right) + 4H\left(\frac{1 - \langle \sigma^z \sigma^z \rangle}{4}\right) - 8H\left(\frac{1 - \langle \sigma^z \sigma^z \sigma^z \sigma^z \rangle}{16}\right) - 4H\left(\frac{1 - 2\langle \sigma^z \sigma^z \rangle + \langle \sigma^z \sigma^z \sigma^z \sigma^z \rangle}{16}\right) - 4H\left(\frac{1 + 2\langle \sigma^z \sigma^z \rangle + \langle \sigma^z \sigma^z \sigma^z \sigma^z \rangle}{16}\right). \quad (20)$$

To reveal the long-range correlation in the system, we study the bonds in the direction that contains the largest distance in the torus, which is marked by a line of elliptic circles in Fig. 1. Without loss of generality, we choose the positions of the bonds as $\mathbf{r}_1 = (0,0)$ and $\mathbf{r}_2 = (0.5L, 0.5L)$ in the $(\mathbf{n}_1, \mathbf{n}_2)$ coordinate system so that the two bonds have the greatest separation. The mutual information between two z linked bonds in this direction is shown in Fig. 7. We find that the mutual information has a maximum at the critical point. This property is valid for different system sizes. The peak values tend to a constant when the system size L trends to infinity.

V. CONCLUSIONS

In this paper, based on the exact ground state of the Kitaev honeycomb model we have obtained both the reduced density matrices of two nearest neighbor sites and between two z linked bonds with the greatest distance. We show that these density matrices have only diagonal elements, so that there is no entanglement between two local sites or two local bonds, but the nonlocal entanglement between one site and the rest of the whole system is maximum. From quantum-information theory, the ground state, which is a multipartite state, seems more like Greenberger-Horne-Zeilinger (GHZ) states other than W -type states. We have calculated the mutual information between two nearest neighbor sites and the mutual information between two z linked bonds with the greatest distance in the torus topology. The first-order derivative of the former mutual information and the latter mutual information itself have peaks at the point where the ground state transits from the gapless phase into a gapped phase. This singular behavior serves as an exact and easily obtainable detector of the topological phase transition in the Kitaev honeycomb model. This *localizable entanglement* is related to the string order parameters and the hidden topological long-range order in one-dimensional spin chains [32,33]. Moreover, the topological phase and topological phase transition have their roots in hidden topological long-range order and the string order parameters. Therefore, investigation of the relation among the localizable entanglement, topological phase transition, and other related quantities in the exactly solvable two-dimensional Kitaev model may greatly enhance our understanding of the topological phase. Research in this direction should be further explored to extensively study the topological phase and topological order by means of quantum information.

ACKNOWLEDGMENTS

This work is supported by grants from the National Natural Science Foundation of China and the 973 program of the Ministry of Science and Technology (MOST), China.

- [1] X. Y. Feng, G. M. Zhang, and T. Xiang, *Phys. Rev. Lett.* **98**, 087204 (2007).
- [2] D. H. Lee, G. M. Zhang, and T. Xiang, *Phys. Rev. Lett.* **99**, 196805 (2007).
- [3] G. Baskaran, S. Mandal, and R. Shankar, *Phys. Rev. Lett.* **98**, 247201 (2007).
- [4] S. Mondal, D. Sen, and K. Sengupta, *Phys. Rev. B* **78**, 045101 (2008).
- [5] K. P. Schmidt, S. Dusuel, and J. Vidal, *Phys. Rev. Lett.* **100**, 057208 (2008).
- [6] S. Dusuel, K. P. Schmidt, and J. Vidal, *Phys. Rev. Lett.* **100**, 177204 (2008).
- [7] J. Vidal, K. P. Schmidt, and S. Dusuel, *Phys. Rev. B* **78**, 245121 (2008).
- [8] G. Kells, J. K. Slingerland, and J. Vala, *Phys. Rev. B* **80**, 125415 (2009).
- [9] J. H. Zhao and H. Q. Zhou, *Phys. Rev. B* **80**, 014403 (2009).
- [10] D. F. Abasto and P. Zanardi, *Phys. Rev. A* **79**, 012321 (2009).
- [11] G. Kells, A. T. Bolukbasi, V. Lahtinen, J. K. Slingerland, J. K. Pachos, and J. Vala, *Phys. Rev. Lett.* **101**, 240404 (2008).
- [12] S. Mandal and N. Surendran, *Phys. Rev. B* **79**, 024426 (2009).
- [13] X. F. Shi, Y. Yu, J. Q. You, and F. Nori, *Phys. Rev. B* **79**, 134431 (2009).
- [14] A. Kitaev, *Ann. Phys. (NY)* **321**, 2 (2006).
- [15] S. Yang, S. J. Gu, C. P. Sun, and H. Q. Lin, *Phys. Rev. A* **78**, 012304 (2008).
- [16] H. D. Chen and Z. Nussinov, *J. Phys. A* **41**, 075001 (2008).
- [17] Z. Nussinov and G. Ortiz, *Phys. Rev. B* **79**, 214440 (2009).
- [18] X. G. Wen, *Quantum Field Theory of Many-Body Systems* (Oxford University Press, New York, 2004).
- [19] H. Yao and S. A. Kivelson, *Phys. Rev. Lett.* **99**, 247203 (2007).
- [20] A. Kitaev, *Ann. Phys. (NY)* **303**, 2 (2003).
- [21] A. Micheli, G. K. Brennen, and P. Zoller, *Nature Phys.* **2**, 341 (2006).
- [22] L. M. Duan, E. Demler, and M. D. Lukin, *Phys. Rev. Lett.* **91**, 090402 (2003).
- [23] Z. Y. Xue, S. L. Zhu, J. Q. You, and Z. D. Wang, *Phys. Rev. A* **79**, 040303(R) (2009).
- [24] J. Q. You, X. F. Shi, X. Hu, and F. Nori, *Phys. Rev. B* **81**, 014505 (2010).
- [25] L. Amico, R. Fazio, and A. Osterloh, V. Vedral, *Rev. Mod. Phys.* **80**, 517 (2008).
- [26] M. A. Nielsen and I. L. Chuang, *Quantum Computation and Quantum Information* (Cambridge University Press, Cambridge, UK, 2000).
- [27] B. Groisman, S. Popescu, and A. Winter, *Phys. Rev. A* **72**, 032317 (2005).
- [28] E. H. Lieb, *Phys. Rev. Lett.* **73**, 2158 (1994).
- [29] J. Cao, X. Cui, Z. Qi, W. Lu, Q. Niu, and Y. Wang, *Phys. Rev. B* **75**, 172401 (2007).
- [30] S. Albererio and S. M. Fei, *J. Opt. B* **3**, 223 (2001); H. Fan, K. Matsumoto, and H. Imai, *J. Phys. A* **36**, 4151 (2003).
- [31] W. Dür, G. Vidal, and J. I. Cirac, *Phys. Rev. A* **62**, 062314 (2000).
- [32] M. Popp, F. Verstraete, M. A. Martin-Delgado, and J. I. Cirac, *Phys. Rev. A* **71**, 042306 (2005).
- [33] H. Fan, Z. D. Wang, and V. Vedral, e-print [arXiv:0903.3791v1](https://arxiv.org/abs/0903.3791v1).